

# Experimental Electronic Structure and Interband Nesting in BaVS<sub>3</sub>

S. Mitrovic,<sup>1,\*</sup> P. Fazekas,<sup>2,3</sup> C. Søndergaard,<sup>1</sup> D. Ariosa,<sup>2</sup> N. Barišić,<sup>2</sup> H. Berger,<sup>2</sup> D. Cloëtta,<sup>2</sup> L. Forró,<sup>2</sup> H. Höchst,<sup>4</sup> I. Kupčić,<sup>5,2</sup> D. Pavuna,<sup>2</sup> and G. Margaritondo<sup>1,2</sup>

<sup>1</sup>*Institut de Physique des Nanostructures, Ecole Polytechnique Fédérale de Lausanne, CH-1015 Lausanne, Switzerland*

<sup>2</sup>*Institut de Physique de la Matière Complexe, Ecole Polytechnique Fédérale de Lausanne, CH-1015 Lausanne, Switzerland*

<sup>3</sup>*Research Institute for Solid State Physics and Optics, Budapest, H-1525 Hungary*

<sup>4</sup>*Synchrotron Radiation Center, University of Wisconsin - Madison, Stoughton, Wisconsin 53589*

<sup>5</sup>*Department of Physics, Faculty of Science, University of Zagreb, HR-10001 Zagreb, Croatia*

(Dated: September 21, 2018)

The correlated 3d sulphide BaVS<sub>3</sub> is a most interesting compound because of the apparent coexistence of one-dimensional and three-dimensional properties. Our experiments explain this puzzle and shed new light on its electronic structure. High-resolution angle-resolved photoemission measurements in a 4eV wide range below the Fermi level explored the coexistence of weakly correlated  $a_{1g}$  wide-band and strongly correlated  $e_g$  narrow-band  $d$ -electrons that is responsible for the complicated behavior of this material. The most relevant result is the evidence for  $a_{1g}$ - $e_g$  inter-band nesting condition.

PACS numbers: 71.30.+h, 71.45.Lr, 79.60.-i

Fundamental arguments as well as the general interest in functional nano-systems justify a broad and increasing interest in electronic phenomena in one dimension. In this context, much attention has been devoted to the correlated transition metal sulphide BaVS<sub>3</sub> that offers the puzzling combination of structural quasi-one-dimensionality with three-dimensional (3D) character of some fundamental electrical and magnetic properties. Reconciling these features is a challenge for condensed matter physics.

The crystal structure can be envisaged as a triangular lattice of chains of face-sharing VS<sub>6</sub> octahedra. Quasi-one-dimensionality is apparent from the fact that V-V distances in the  $a$ - $b$  plane (6.72Å) are almost 2.4 times as large as in the  $c$ -direction of chains (2.84Å). Naively, one would expect good metallic conduction along the chains, and poor conduction in the perpendicular directions. Indeed, this was the prevalent view of the nature of BaVS<sub>3</sub> as long as only polycrystalline samples were available [1]. The first resistivity measurements on single crystal samples [2] showed that in a wide range of temperatures, conductivity is essentially isotropic ( $\sigma_c/\sigma_a \sim 3$ ). This required a re-examination of the effective dimensionality of BaVS<sub>3</sub>, and its relationship to the correlation phenomena displayed by the system.

A salient feature of BaVS<sub>3</sub> is the second-order metal-insulator transition (MIT) at  $T_{\text{MI}}=69\text{K}$ , which is manifested also in a strong susceptibility cusp. In most two- or three-dimensional transition metal compounds, the MIT is accompanied by a magnetic, or a structural transition. However, BaVS<sub>3</sub> is exceptional. The phase on the low- $T$  side of the MIT is non-magnetic, and the structural aspect of the MIT was long overlooked until the recent discovery of tetramerization (doubling of the unit cell in the  $c$ -direction) [3].

BaVS<sub>3</sub> is a  $3d^1$  system with intermediate strength

of correlations [4]. Local correlations are not strong enough to sustain a paramagnetic insulating phase in high-quality undoped samples [2, 5]. The  $T > T_{\text{MI}}$  phase is metallic but certainly a correlated metal: the susceptibility is Curie-like, showing that a substantial fraction of the V sites carries a local moment [2, 6]. The MIT should be characterized as a Mott-Slater transition [4]: a symmetry breaking transition assisted by correlations. The fact that the MIT must be accompanied by symmetry breaking, was deduced from the observation that the MIT remains a continuous phase transition in a wide range of pressures [4, 7], prior to the experimental identification of the only known candidate for order parameter: the tetramerization [3].

Before proceeding, we would like to mention that BaVS<sub>3</sub> has two other phase transitions: a hexagonal-to-orthorhombic structural transition at  $T_S = 250\text{K}$  [1, 6], and the onset of antiferromagnetic long range order at  $T_\chi = 30\text{K}$  [2, 6, 8]. The role of the orthorhombic splitting will be discussed elsewhere [9], while we neglect it in our discussions of the ARPES data. Our results are taken at  $T_\chi < T < T_S$ , on both sides of the MIT.

The difficulties of interpreting the properties of BaVS<sub>3</sub> are partly due to the unclear character and occupancy of the relevant  $d$ -states. In the ionic picture of a single  $V^{4+} = 3d^1$  site surrounded by a distorted octahedron of S sites, the trigonal component of the crystal field splits the  $t_{2g}$  level into the non-degenerate  $a_{1g}$ , and the doubly degenerate  $e_g$  level. If  $e_g$  states are occupied, the interplay of orbital and spin degrees of freedom is important.

Hopping processes broaden the levels into the corresponding  $a_{1g}$  and  $e_g$  bands. Now the question is whether both bands are partially occupied or it is sufficient to consider one band only. If only the  $a_{1g}$  band counts, the insulating phases of BaVS<sub>3</sub> must be describable in terms of atomic displacements and spins. If only  $e_g$  states are

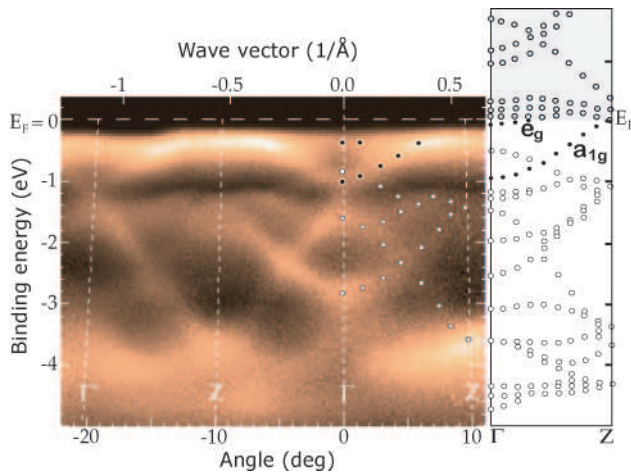


FIG. 1: (Left) ARPES intensity map taken in the direction parallel to structural chains at 40K. Brighter color signifies higher intensity. Bands arising from the  $V(3d)$  level are followed with black circles, and the  $S(3p)$  bands with the white ones. The spectra were normalized and a background was subtracted to enhance the features. (Right) Corresponding theoretical band dispersion from Ref. [10]

occupied, spin and orbital ordering must be considered on an equal footing (a preliminary discussion of this scenario was given in [2]). If both  $a_{1g}$  and  $e_g$  electrons are present, complicated scenarios can arise.

Choosing the orthorhombic  $c$ -axis as the  $z$  axis, the  $a_{1g}$  orbital has  $z^2$  character, with strong overlap in the  $c$ -direction. The  $a_{1g}$  band is wide and almost one-dimensional. If only the  $a_{1g}$  band were filled,  $\text{BaVS}_3$  could be an ordinary semiconductor or a weakly correlated metal, without the possibility of localized moment formation. This is obviously not the case. There must be also  $e_g$  electrons. In fact, all band structure calculations [10, 11, 12] agree that the Fermi level is lying in the region of the crossing of  $a_{1g}$ -like and  $e_g$ -like bands. However, the status of these predictions is somewhat uncertain because neither of the calculations yields the possibility of a non-magnetic insulating state. It is important to have experimental results about the filling of the  $e_g$  and  $a_{1g}$  bands, and the nature of the electronic structure in the intermediate ( $T_X < T < T_{\text{MI}}$ ) insulating phase.

For many years, angle-resolved photoemission (ARPES) has been used to experimentally probe the electronic band structure of different materials. This powerful approach, however, requires high quality single crystals of reasonable size. We were able to grow suitable crystals for  $\text{BaVS}_3$  to experimentally determine the band structure and therefore to provide a solid background for the understanding of this compound. The most relevant result is the indication that the MIT is associated with interband nesting.

We performed ARPES on fairly large ( $\approx 0.25 \times 0.25 \times 3$  mm<sup>3</sup>) single crystals of  $\text{BaVS}_3$  grown by the slow cool-

ing technique in melted Tellurium [13]. The data were collected at the PGM beamline of the SRC, Stoughton (WI), USA, and with a Scienta-2002 analyzer. The spectra presented were measured with a total energy and momentum resolution of  $\Delta E = 15\text{meV}$  and  $\Delta k = 0.04 \text{ \AA}^{-1}$ . Clean surfaces were exposed in UHV conditions of the analyzer chamber ( $10^{-11}\text{mbar}$  range). The temperature of the sample could be controlled in the range from 5K to 150K.

Due to the pronounced one-dimensional structure, samples were fractured rather than cleaved and made momenta of electrons poorly defined in perpendicular-to-chain direction. The measurements in the parallel-to-chain direction, however, were successfully reproduced every time.

Fig. 1 shows the ARPES intensity map taken in the  $\Gamma$ - $Z$  direction parallel to the chains. For best resolution, measurements were taken at  $T = 40\text{K}$ , and with a photon energy of 50eV, where we found all features close to the Fermi level  $E_F$  distinctly resolved. A corresponding part of the *ab initio* calculation for the orthorhombic phase by Mattheiss [10] is displayed next to the map. The measured intensity maps are essentially unchanged from 40K to 150K, except for the temperature broadening of the features and the shift of the leading edge close to the Fermi level as discussed later.

The theoretical  $\mathbf{k}$ -space periodicity in the extended zone scheme is well reproduced in Fig. 1, indicating that the measured surface gives a good probe for the bulk states. We read off the period  $2z$  where  $z = \overline{\Gamma Z} \approx \pi/c_0 = 0.56 \text{ \AA}^{-1}$ ,  $c_0 = 5.61 \text{ \AA}$  being the  $c$ -axis lattice constant for the two-atomic unit cell.

We find that both the positions and the widths of the bands at energies above 1eV - originating from the  $S(3p)$  orbitals - are in agreement with the calculations [10].

Details of the electronic states just below the  $E_F$  are shown in the  $-d^2I/dE^2$  intensity map of Fig. 2(c). The second derivative clearly reveals two bands: a dispersive band with  $\lesssim 1\text{eV}$  bandwidth, which we identify as a one-dimensional  $a_{1g}$  band; and an apparently rather non-dispersive band located at  $\sim 0.4\text{eV}$ , which we associate with  $e_g$  states. Selected raw measured energy distribution curves (EDCs) presented in the Fig. 2(d) also demonstrate both features. This analysis only crudely determines the band structure close to the Fermi level. A different approach is needed, and discussed in the following paragraph, to resolve the structure in the closest proximity of the  $E_F$ , essential for the transport properties.

A previous photoemission study reported the results of angle-integrated measurements on polycrystalline samples [14]. Our angle-resolved results on good single crystals confirm the previous findings about the lack of a Fermi edge in a temperature range above  $T_{\text{MI}}$ . In our ARPES maps, peaks of all bands fail to cross the

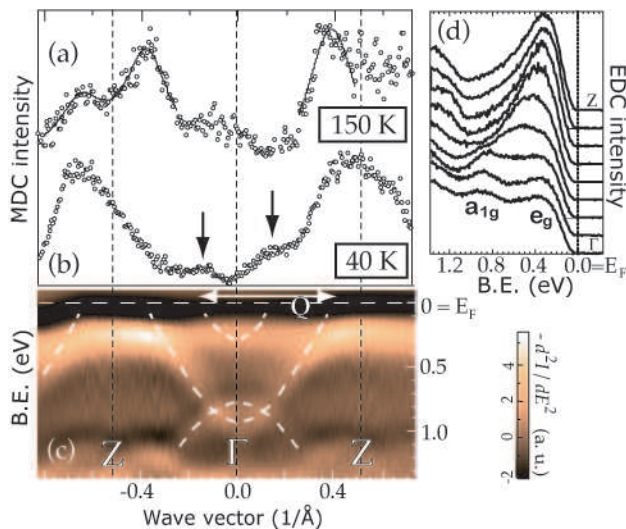


FIG. 2: (a) An MDC of 50meV wide integrated region just below the Fermi energy ( $E_B^* = 50\text{meV}$ ) from an ARPES map at 150K. The fit is a double Lorentzian. (b) The equivalent MDC plot ( $E_B = E_B^* - 80\text{meV}$ ) from a map at 40K. The arrows indicate the positions of  $k_{F_2}$ . (c)  $-d^2I/dE^2$  plot of the ARPES map at 40K. The dashed lines serve as guides to the eye. (d) Selected raw EDC's in equidistant steps from  $\Gamma$  to Z point.

Fermi level even in the metallic state. This was previously attributed to Luttinger-liquid behavior. However, the electronic properties of  $\text{BaVS}_3$  are too far from being quasi-1D to permit such an interpretation. On the other hand, we note that such spectroscopic features are not unusual in correlated electron systems (Ref [15] and therein). Spectral weight, which is the only observable of an ARPES experiment, is often renormalized by strong interactions which can shift the spectral weight to higher binding energy masking the real quasiparticle peak. Fermi level crossing is often still observable with careful analysis. For that purpose we took a momentum distribution curve (MDC) from an ARPES map taken at 150K with a 50meV wide window of integration around the Fermi level. The obtained MDC shown in Fig. 2(a) reveals peaks marking the crossings of the  $a_{1g}$  band within the first and the second Brillouin zone. The crossing determined from Lorentzian peak fits, takes place at the wave vector  $k_{F_1} = (0.40 \pm 0.05) \text{\AA}^{-1}$ . The symmetry of the crossings from both sides of the BZ positions the point  $Z = (0.56 \pm 0.05) \text{\AA}^{-1}$ , in agreement with the theoretical value.

The  $e_g$ -band is not so well resolved. However, the increase in intensity not far from the  $\Gamma$  point in Fig. 2(a) indicates the possibility of a Fermi level crossing, creating a shallow electron pocket. If we look at the equivalent MDC in the low temperature map (Fig. 2(b)) that accounts for the spectral changes due to the gap opening, the electron pocket shape of the band is clearer. The

band should cross  $E_F$  at  $k_{F_2} = (0.15 \pm 0.05) \text{\AA}^{-1}$ . The electron pocket shape is in agreement with the theoretical predictions.

The apparent bending of the  $e_g$  band towards the  $a_{1g}$  band is a consequence of the resolution and back-folding of *shadow* bands – the signature of lattice distortions [15]. Equally, the  $a_{1g}$  band folds into shadow bands, which is the reason behind the high intensity around the Z point since the signals from both sides of the Brillouin zone boundary overlap.

We cannot see the higher-lying part of the  $a_{1g}$  band (see Fig.1 (right)) but its overall width must approach the theoretical value  $W(a_{1g}) \sim 2\text{eV}$ . On the other hand, we estimate  $W(e_g) < 0.4\text{eV}$ . We conclude that the intriguing behavior of  $\text{BaVS}_3$  results from the fact that two kinds of  $d$ -states: strongly correlated narrow-band  $e_g$ -states, and weakly correlated wide-band  $a_{1g}$ -states, coexist at the Fermi level.

Clearly, the transport properties, including the observed low anisotropy, should originate from both bands that cross the  $E_F$ . Indeed, the estimate of the ratio of averaged Fermi velocities [10], obtained supposing band structure similar to our findings, gives  $\langle v_{\parallel}^2 \rangle / \langle v_{\perp}^2 \rangle \propto \sigma_c / \sigma_a \sim 3.8$ , in close agreement with the experimental result [2]. New calculations based on our experimental data find the same ratio [9]. In addition, our data show that the  $a_{1g}$  band is hybridized with one of the sulphur  $\pi$  bands, which should play a role in reducing the macroscopic manifestation of the quasi-1D crystal structure.

We ascribe the Curie-like susceptibility, and the bad metallic character of the  $T > T_{\text{MI}}$  phase, to  $e_g$  electrons, and to  $e_g$ - $a_{1g}$  scattering. As to the symmetry breaking aspect of the MIT, the orbital degrees of freedom of the  $e_g$  electrons are expected to give an electronic order parameter complementary to the structurally defined tetramerization amplitude. Spin-orbital models have the capacity to describe the development of a spin gap, which is known to accompany the MIT of  $\text{BaVS}_3$  [16].

Strong one-dimensional structural fluctuations are observed in a wide temperature range above the MIT in diffraction experiments [17]. Such observations are common in quasi-1D charge density wave (CDW)-bearing systems. However, a CDW is only one of the DW states  $\text{BaVS}_3$  can support, and the CDW is likely to be accompanied by the modulation of orbital character. Nevertheless, as in CDW systems, the 1D fluctuations ought to have a relation to  $\mathbf{k}$ -space features. We examined our experimentally determined band structure to check if we can identify a Fermi surface instability which can introduce a gap into the wide  $a_{1g}$  band.

We find that the  $a_{1g}$  band alone cannot satisfy the nesting condition, thus we exclude intra-band nesting. We can also exclude a  $4k_F$  instability, or the possibility of the  $e_g$  band supporting nesting in itself. On the other hand, our results are consistent with an instability involv-

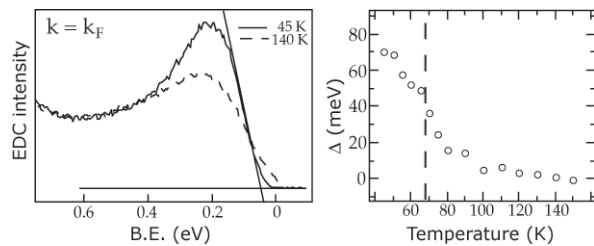


FIG. 3: (Left) EDC's taken at 140 and 45K at the  $E_F$  crossing of the  $a_{1g}$  band. The method of leading edge position extraction is shown on the low-temperature EDC and (Right) is its dependence on the temperature. The dashed line in (right) marks the MIT temperature.

ing both bands, since our data are in agreement with a condition  $k_{F_1} + k_{F_2} = 0.5c^* = Q_{CDW}$ . The mechanism of interband nesting leading to a CDW insulating state is known in low-dimensional systems such as quasi-1D organic conductors and  $K_{0.3}MoO_3$  blue bronze. However, the nature of the  $T_\chi < T < T_{MI}$  phase of  $BaVS_3$  is not yet clear, and the precise mechanism of the instability involving both kinds of bands remains to be identified.

We have monitored the spectral changes with temperature through the MIT. The position of the peak in the EDCs of our intensity maps (Fig. 3) stays at the same position but the leading edge moves to higher binding energies. If we plot the position of the leading edge versus temperature, we see a monotonic shift of the leading edge - that most probably started above 150K - and a noticeable non-linear increase in the shift below 90K. This is consistent with the results of Ref. [14] and indicative of the opening of a charge gap. We do not see a clear transition associated with the  $T_{MI} = 69K$ . This is not unusual, particularly when pre-transitional fluctuations are present. The gap as seen in photoemission spectra develops in the same range of temperature where resistivity [2, 7] and thermopower [18] measurements identify a "precursor" to the insulating phase, and where X-Ray diffraction detects large 1D fluctuations [17]. The saturation of the leading edge shift indicates a charge gap of  $\Delta_{ch} = 60 - 70meV$ . This is in good agreement with the value obtained from transport measurements in the temperature range where the Arrhenius law applies [2, 6, 14].

We point it out that the gap opening can be seen for any choice of  $k$  vector, as should be expected if the complete Fermi surface participates and if we take into account that the closeness of the bands and surface-defined momentum resolution smear out signals from both bands across the Brillouin zone.

The broad, pseudogapped spectral features are incompatible with a standard quasiparticle picture. Recently, it was argued that in Peierls systems they are a signature of polaronic carriers. The strong case for this scenario was found in the studies on  $K_{0.3}MoO_3$  blue bronze [15].

Analogous considerations may hold for  $BaVS_3$ , where the MIT has certain aspects of a spin-Peierls transition, and the coupling of the  $e_g$  electrons to the local Jahn-Teller modes is important. Interpretation of spectra in terms of Luttinger liquid or signal overlap from multiple bands is unlikely, since similar consideration for blue bronze were eliminated through studies on the related insulating, "one-band" system  $K_{0.33}MoO_3$  (red bronze) [15].

To conclude, we derived the structure of the bands close to the Fermi level from ARPES measurements in a wide range of temperatures on both sides of the MIT at 69K. We found that the physics of  $BaVS_3$  is governed by the coexistence of weakly correlated wide-band  $a_{1g}$  electrons and strongly correlated narrow-band  $e_g$  electrons near the Fermi level. Our results are consistent with the  $a_{1g}$ - $e_g$  interband nesting condition and we propose it as a plausible mechanism for the metal-insulator transition.

The authors are grateful for illuminating discussions to T. Fehér and S. Barišić. Initial measurements were performed at ISA, University of Aarhus, Denmark, and we are grateful to P. Hofmann for this opportunity. The SRC, UW - Madison, is supported by the NSF under Award No. DMR-0084402. This work was supported by the Swiss National Science Foundation through the MaNEP NCCR. P.F. acknowledges support by the Hungarian National Grant T038162.

*Note added.* The results of a recent LDA+DMFT calculation by F. Lechermann et al (cond-mat/0409463) about the role of correlations in determining the electron distribution over  $a_{1g}$  states are in good overall agreement with our experimental findings.

---

\* Electronic address: slobodan.mitrovic@epfl.ch

- [1] O. Massenet et al., Mat. Res. Bull. **13**, 187 (1978)
- [2] G. Mihály et al., Phys Rev B **61**, R7831 (2000).
- [3] T. Inami et al., Phys. Rev. B **66**, 073108 (2002).
- [4] P. Fazekas et al., Physica B **312-313**, 694 (2002).
- [5] A. Gauzzi et al., Int J Modern Phys B **17**, 3503 (2003).
- [6] T. Graf et al.: Phys Rev B **51**, 2037 (1995).
- [7] L. Forró et al., Phys Rev Lett **85**, 1938 (2000).
- [8] H. Nakamura et al., J. Phys. Soc. Japan **9**, 2763 (2000)
- [9] I. Kupčić, S. Barišić, to be published.
- [10] L.F. Mattheiss, Solid St. Commun. **93**, 791 (1995).
- [11] X. Jiang and G.Y. Guo, Phys Rev B **70**, 035110 (2004)
- [12] M.-H. Whangbo, H.-J. Koo, D. Dai, and A. Villesuzanne, J Solid State Chem **165**, 345 (2002); *ibid* **175**, 384 (2003).
- [13] H. Kuriyaki, H. Berger, S. Nishioka, H. Kawakami, K. Hirakawa, and F.A. Lévy, Synthetic Metals **71**, 2049 (1995)
- [14] M. Nakamura et al., Phys Rev B **49**, 16191 (1994)
- [15] L. Perfetti et al., Phys Rev B **66**, 075107 (2002); S. Mitrovic et al., Phys Rev B **69**, 035102 (2004)
- [16] I. Kézsmárki et al., Phys Rev B **63**, 081106(R) (2001).
- [17] S. Fagot et al., Phys Rev Lett **90**, 196401 (2003).
- [18] N. Barišić et al., to be published.